

A real time measurement of junction temperature variation in high power IGBT modules for wind power converter application

Pramod Ghimire¹, Kristian Bonderup Pedersen², Angel Ruiz de Vega¹, Bjørn Rannestad³, Stig Munk-Nielsen¹, Paul Bach Thøgersen³

¹Department of Energy Technology, Aalborg University, Denmark

²Department of Physics and Nanotechnology, Aalborg University, Denmark,

³kk-electronic a/s, Denmark

Abstract

This paper presents a real time measurement of on-state forward voltage and estimating the junction temperature for a high power IGBT module during a power converter operation. The power converter is realized as it can be used for a wind turbine system. The peak of the junction temperature is decreased at higher fundamental frequency due to change in on-state time from the change in output frequency. The junction temperature is estimated using the on-state collector-emitter voltage of the IGBT module. Lower output frequency is thermally a higher stressing zone for wind power converters, hence the low frequency range is considered from 6Hz to 20Hz; the corresponding on-state collector-emitter voltage and junction temperature are presented. The estimation of junction temperature is compared with finite element based thermal simulations. The peak temperatures at different frequencies are compared between measurement and simulation results. The measurement technique designed to be implementable for field application.

1 Introduction

Wind turbine technology is growing rapidly since its instalment in 1980s [1]. Due to the intermittent nature of wind, grid code requirements and the high power density, the power electronic converters suffer mostly to fulfill reliability issues [2, 3].

Power transistors are expensive and most vulnerable part in wind power converters for higher oscillating junction temperature. Silicon based multichip Insulated Gate Bipolar Transistor (IGBT) power modules are mostly in use, which have weak capability against high amplitude thermal cycle. In fact, the hardness of the silicon causes the failures due to higher thermo-mechanical stress [4]. Generally, solder degradation and bond wire lift-off are the major failures in multi-layer modules [5]. A number of IGBTs are mounted in one converter depending upon the converter topology [2]. A survey conducted on offshore wind turbine technology shows that power modules are the most vulnerable part in their electrical system [6, 7].

In comparison to traction application, a real time monitoring is more rare in wind power converters [8]. In order to avoid the catastrophic failure of the device and to improve the total reliability of power converters, an online monitoring method may play a vital role in power converters. In regards to IGBTs, the major electrical-thermal parameter such as thermal impedance, gate threshold voltage, gate capacitance, collector emitter voltage etc. are considered as ageing parameters [5, 9-10]. A deviation in those parameters such as 10-20% increment on V_{ce} , may be used as failure criteria for the transistor [11]. Out of those parameters, a temperature sensitive parameter (TSEP) which in this case is the on-state collector-emitter voltage (V_{ce}): is used to estimate the junction temperature of the IGBT while the converter is in operation [12].

This paper presents a method to measure the on-state V_{ce} while the converter is in operation. In order to realize a

real life application, a wind power converter is used and the measurement is conducted at lower frequency range from 6Hz to 20Hz. Operating at lower frequency range increases thermal stress to the power module due to power losses over longer time period. Especially, in case of a doubly-fed induction generator (DFIG), the inverter has to deliver excitation energy at a frequency from 0Hz to 16Hz [8]. The converter is thermally stressed and has proven the weakest part in terms of reliability for wind power converters. Therefore, a focus is given in the thermal stressing zone.

2 IGBT power module

The power module consists of multi-layers of different packaging materials with unmatched coefficient of thermal expansion (CTE). The junction temperature monitoring is important because the major failures such as bond wire fatigue, solder joint fatigue etc. are dependent on thermal loading such as temperature swing, mean temperature and electrical parameters. [11].

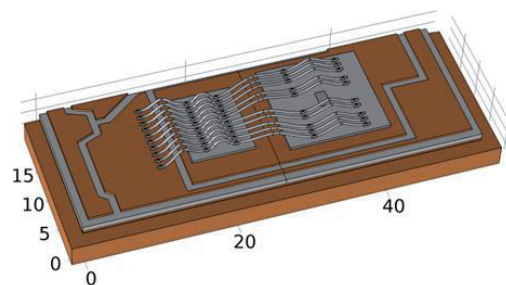


Figure 1 CAD figure showing one section of a module. The section consists of one IGBT chip, one diode chip and 10 bond wires.

A 1700V/1000A IGBT power module is used as a device under test module. The module consists of identical sections each with two IGBT chips, two diodes, and 20 bond wires. Apart from this it is an ordinary direct copper bonded (DCB) substrate with an *AlN* ceramic, large *Al* wires, and a *Cu* baseplate. The geometry is depicted in Figure 1 and the thickness of the various layers is seen in Table 1.

Material	Thickness [μm]
Bond wire – <i>Al</i>	400
Metallization – <i>Al</i>	3
Chip – Diode/IGBT	300
Die attach – solder paste	50
Copper	300
Ceramic – <i>AlN</i>	700
Copper	300
DCB attach – Solder paste	100
Baseplate – <i>Cu</i>	3000

Table 1 Vertical layers of the IGBT module with layer, thickness and composition

3 Power converter

An H-bridge topology is used as a converter where half bridge IGBT modules are used on each leg as depicted in Figure 2 [13]. One leg is used as a device under test (DUT) and the other is used as a control side in order to control the power flow. In the control side, two legs are used to share the current from the DUT. This ensures the IGBT modules of the control side to not wear-out prior to the DUT.

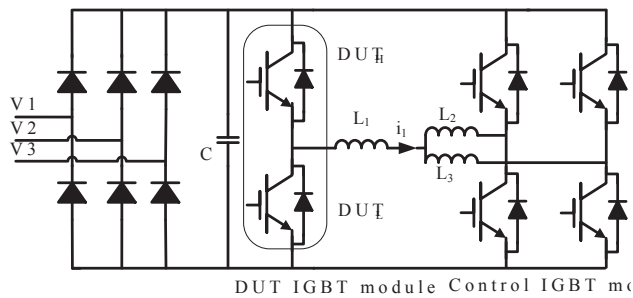


Figure 2 A power converter topology

Where,

DUT_H: High side of device under test IGBT module

DUT_L: Low side of device under test IGBT module

L₁, L₂, L₃: Load inductors

The power converter operating parameters are shown in Table 2.

Parameter	Value
DC link voltage (V_{DC})	1000V
Output voltage (V_{out})	315Vrms
Load current (I_L)	630Arms

Parameter	Value
Fundamental frequency(f_{out})	6Hz
Switching frequency (f_{sw})	2.5kHz
Water temperature for cooling	80°C

Table 2 The converter operating electrical parameters

4 Measurement technique

As discussed before, an on-state V_{ce} is chosen as an ageing and temperature monitoring parameter. As the DC-link voltage is 1000V, so during switching period the collector-emitter voltage swings between less than 1V to 1.14KV due to transient loading as illustrated in Figure 3. Hence, the circuit should have featured with high blocking voltage with a very good accuracy.

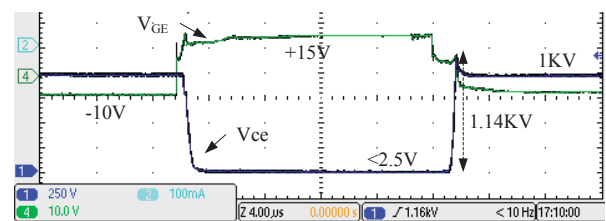


Figure 3 A V_{ce} turn on/off waveform and transient during switching

In addition to this, the on-state voltage has transient behaviour during turn-on time due to dynamics of the switching. Hence, the voltage measurement circuit should measure the voltage after completing the transient region as shown in Figure 4 to increase the accuracy of the measurement. Approximately, the on-state voltage has dynamics for the first 12μs in the tested IGBT module as illustrated in Figure 4.

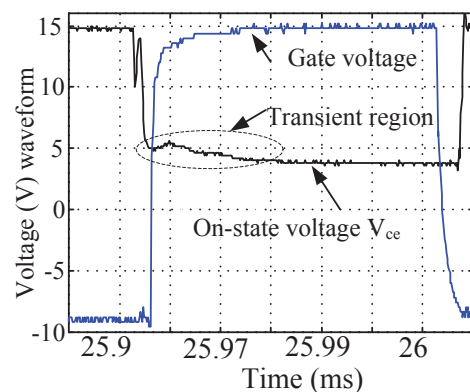


Figure 4 Gate emitter voltage waveform and V_{ce} voltage waveform measured at V_{b1}

4.1 Voltage measurement

The circuit is built to measure the on-state V_{ce} and V_{FD} during the converter operation. A single circuit is able to measure both high and low side IGBTs and diodes of the DUT. Details of the circuit are described by Szymon et al. [14]. The circuit is built to be operational in real life ap-

plications. Figure 5 shows the measurement circuit used to measure the V_{ce} .

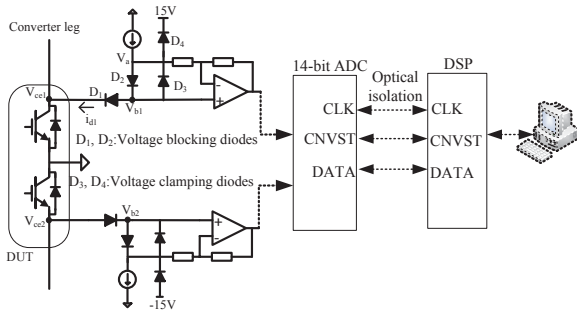


Figure 5 A V_{ce} measurement circuit

Two diodes are connected in series and a weak current source is forward-biased them during IGBT turn-on time as given in Figure 5. When the IGBT is off, the diode D_1 is blocked the V_{ce} voltage.

$$V_{ce1} = V_{b1} - V_{D2} = V_{b1} - (V_a - V_{b1}) = 2V_{b1} - V_a \quad (1)$$

Assuming that the two diodes are identical $V_{D1} = V_{D2}$, the V_{ce} is measured by subtracting the voltage drop on D_2 from V_{b1} potential as given in Equation 1. V_{D1} and V_{D2} are voltage across D_1 and D_2 respectively. The measurement part of the circuit is isolated using an optical fibre connection with the rest of a data logging system.

5 Junction temperature estimation

Junction temperature monitoring is of a paramount interest to improve the total reliability of power converters. A calibration of $V_{ce}-T_j$ is conducted to obtain a calibration factor at higher current levels in the converter itself. A time is taken in account to rise up the current and to fall at zero level during the calibration process. The coolant temperature is maintained at a constant value during the measurement process. Finally, the junction temperature is calculated based on the real time measurement of the on-state voltage and the calibration factor.

5.1 $V_{ce}-T_j$ Calibration

Initially, the on-state V_{ce} and T_j are calibrated at temperatures ranging from 22°C to 80°C for up-to 960A_{peak}. The baseplate temperature is kept homogeneously distributed by using Danfoss shower power [15] and by controlling the coolant temperature. A self-heating of the power converter is used to increase the coolant temperature.

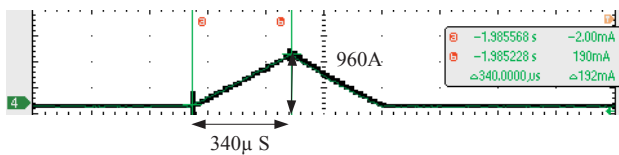


Figure 6 A current waveform during calibration

During the calibration process a normal PWM switching of the converter is turned off. The current i_1 is ramped up

through the inductors and the respective current and on-state voltage for IGBTs and free-wheeling diodes are measured as shown in Figure 6.

Each calibration process takes 680μs at one temperature level. Figure 7 (a) shows the $V_{ce}-T_j$ calibration and Figure 7 (b) shows a calibration factor for IGBT module at different current levels.

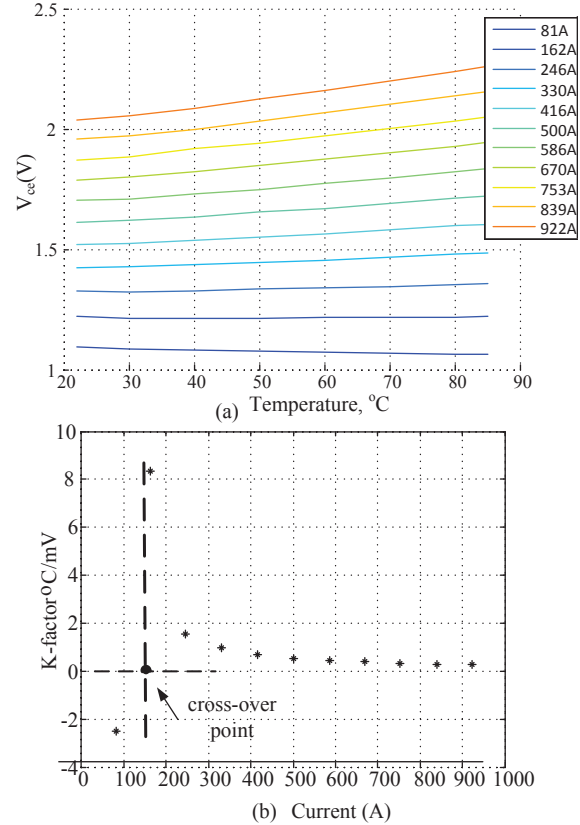


Figure 7 A $V_{ce}-T_j$ calibration (a) $V_{ce}-T_j$ calibration at different current level (b) A calibration factor for IGBT

6 Thermal Simulation

The thermal modeling contains two interconnected problems, namely the power loss inside the module and the distribution of heat. The power loss and temperature problems are interconnected e.g. through the temperature dependence of physical parameters like the electric and thermal conductivity. But even more so through the complex non-homogeneous fields created inside power modules by transient loads [16-17].

In the following section a finite element method (FEM) is presented for the evaluation of the temperature field as a function of time. The derived results are compared to the temperature measured online. The model presented is based on the work carried out in [17], where everything is presented in detail. In the present only relevant data is included.

6.1 Physical parameters

In modern FEM based simulations one of the governing factors are the physical parameters [18]. With regards to pure materials like the *Al* wires and the *Cu* pads this is a simple matter, however, the IGBTs and the diodes are in principal non-linear and non-isotropic structures which are not ideal for continuum assumptions. This is solved by using so-called effective medium parameters for the elements representing the semiconductor chips in the calculations. This is presented and discussed in detail in [19] and [17]. For all materials, temperature dependent parameters are introduced for vital coefficients like the thermal and electrical conductivity.

6.2 Power loss

The power loss inside the module may roughly be divided into conduction-, switching-, and gate loss: where the last one is normally neglected: [19]

$$P_{tot} = P_{cond} + P_{sw} + P_{gate} \approx P_{cond} + P_{sw} \quad (2)$$

The conduction loss is an ordinary ohmic contribution which affects all current carrying components of the geometry in Figure 1, namely the DCB, wires, chips, and solders.

6.2.1 Conduction Loss

All contributions from the conducting metals of the geometry are considered evenly distributed and are calculated from the electrical conductivity of pure materials. The semiconductors on the other hand are more complicated as discussed in the previous section as these are non-isotropic, non-linear materials. The IGBTs consists of a large amount of parallel transistor channels, which ideally are identical. In a similar way the diode acts as a channel as well. All conducting channels of the semiconductors are assumed to perform evenly, and the only changes in the current distribution allowed are created by the temperature fields. Apart from that the power loss is calculated based on datasheet specifications.

6.2.2 Switching Loss

The switching loss is a phenomenon only observed in the semiconductor chips. In the IGBT, the switching loss includes the energy required to switch on and off the component, whereas in the diode only the so-called recovery loss is included [21].

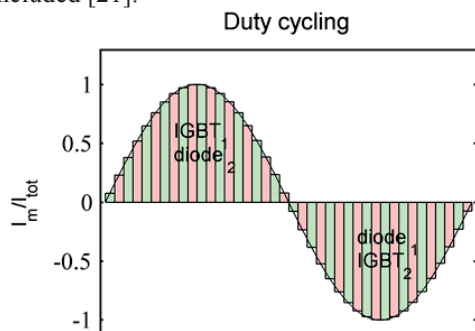


Figure 8 Current load experienced by the power module

In Figure 8, the duty cycle load applied to the module is illustrated. The current attains a sinusoidal waveform which accordingly yields the sinusoidal on-state voltage as shown in Figure 12. Each of the color bars in Figure 8 symbolize a switching period of time: $t_{sw} = t_{on} + t_{off}$. In Figure 9, the power loss in a single period for one IGBT chip is illustrated. As illustrated the switching loss is in principle placed initially and in the end of the period, when switched on and off respectively. In the present, the switching loss is assumed evenly distributed during the on-state time t_{on} and considered constant P_{swm} in the given on-state.

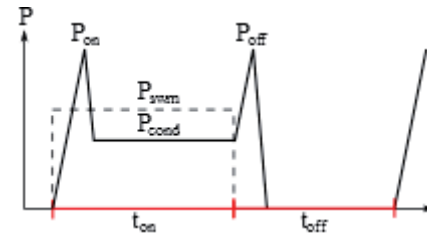


Figure 9 Power loss in a single IGBT chip during one switching cycle [20].

6.3 Thermal model and boundary conditions

The FEM simulation in principle only concerns solving the convection-diffusion-reaction problem as described in [16-17]. Solvers, meshing, and geometrical specifications are carried out and specified in COMSOL multiphysics. Therefore one of the primary assignments, as discussed in [16], is to specify the proper boundary conditions.

Baseplate cooling is one of the governing factors apart from the power loss. As mentioned in Section 5.1, the baseplate is water-cooled directly using Danfoss shower-power. Based on the pumping capacity as well as the mixture of water and glycol the convection coefficient h_{SP} can be obtained from [21], so that the normal heat flux out of the baseplate may be calculated as given in Equation (3):

$$q_n = h_{SP}[T_{water} - T(x, y)] \quad (3)$$

Here the water temperature is assumed constant across the baseplate and over time. This assumption is supported by measuring the cooling water temperature over time which is kept close to 80°C. From Figure 1, it is clear that only a reduced geometry is considered. Out of the six sections only half a section is regarded. This means that interactions between individual sections and the two halves of a section need to be included in the boundary conditions. The former is assumed to only affect the medium temperature of the section as the primary power is dispersed towards the backside of the baseplate. This is accounted for through fitting to the experimental data. The latter interaction, however, is more complicated. As the missing part of the section is an inverted mirror of the part illustrated the total power passing through the plane separating them will be the same. The flux field, however, will be inverted in the same way as the geometry. This is included simply by adding the outgoing flux from the IGBT and the diode

respectively as an ingoing flux half a period later with a correction with respect to the inversion. The remaining boundary conditions are kept simple to speed up calculations. This means that the silicone gel covering the components is treated as a passive convection surface. And all inside connections are assumed ideal.

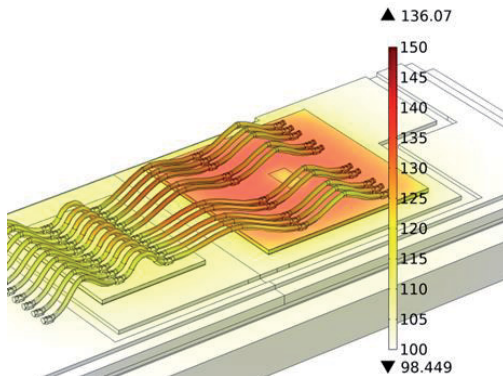


Figure 10 Temperature field at the peak IGBT temperature at an output frequency of 6Hz

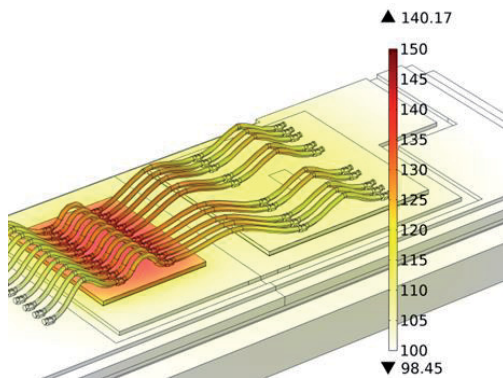


Figure 11 Temperature field at the diode peak temperature at an output frequency of 6Hz

6.4 Temperature curves

The used conditions for the simulations are the same as listed in Table 1. With the mentioned conditions for the simulations 30 cycles had to be computed before reaching the equilibrium period. With respect to resolution of meshes and time stepping it was refined until conversion of the final result. In Figure 10 and 11, the surface temperature field of the diode and IGBT chips are presented at their peak values. The simulation is carried out at a 6Hz output frequency. As would be expected the temperature is significantly higher in the center of the chips and decreases towards the edges. This illustrates one of the difficulties of working with online measuring of the temperature as the peak value differs significantly from the mean junction temperature, as illustrated in Figure 14.

7 Measurement and simulation results

The online measurement is conducted from 6Hz to 20Hz on every 2Hz increment. The on-state V_{ce} and V_{FD} are measured for the high side IGBTs and diodes respectively as shown in Figure 12.

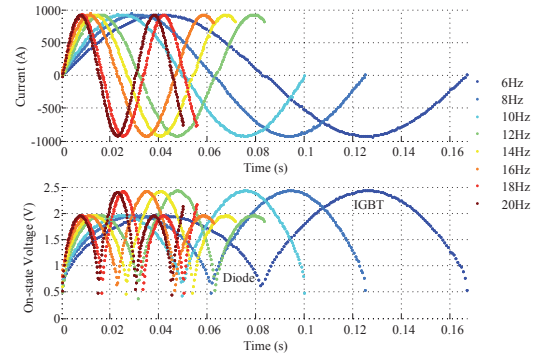


Figure 12 A measured on-state V_{ce} from 6Hz to 20Hz for IGBTs and diodes

The on-state voltage when the current at 920A is compared and found that the V_{ce} is closely 10mV less in low side IGBT at 20Hz than the 6Hz frequency. The junction temperature is calculated for different frequencies as shown in Figure 13.

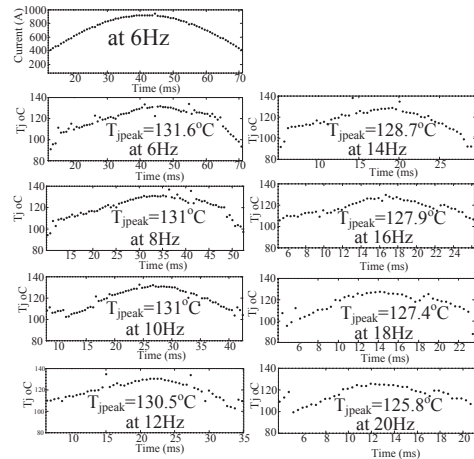


Figure 13 A measured peak temperature variation at different frequency

The peak temperature variation for IGBTs at 6Hz to 20Hz frequencies are shown in Figure 14 for measured and thermal simulated results. As seen in the figure, it is clear that both results fairly match the peak and temperature variation on each half cycle.

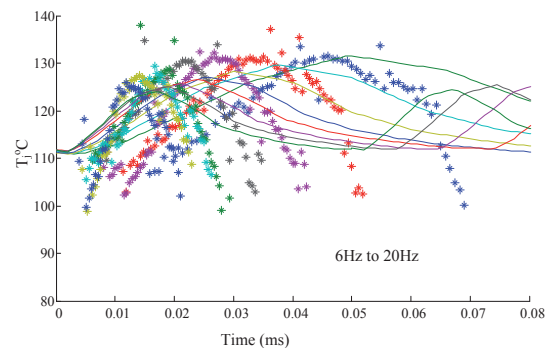


Figure 14 A T_j variation in measured and simulation compared together for 6Hz to 20Hz

To illustrate more in comparison between two studies, only peak temperature variations on each frequency are plotted in Figure 15. The peak temperatures T_j are very

close. In conclusion, the peak junction temperature drops 131.6 to 125.8 which is 5.8°C from 6Hz to 20Hz in the measurement.

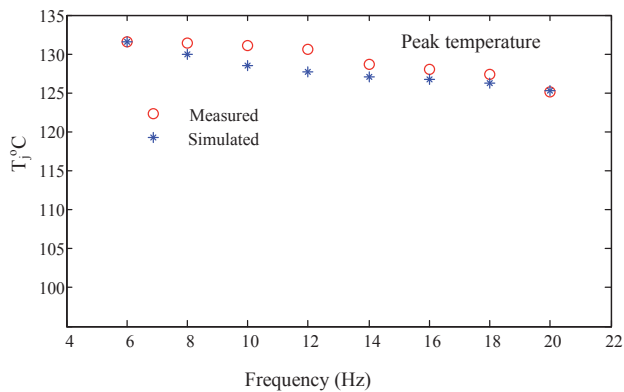


Figure 15 A comparison of peak T_j between measured and simulation

8 Conclusion

The junction temperature is monitored in real time while a power converter is in operation and the peak temperature is increased by approximately 5.8°C from 20Hz to 6Hz application for a 1700V and 1000A module. The thermal analysis using FEM simulation is conducted and peak temperature variation fairly matches between measurement and simulated results. This measurement technique is less complex and easy to implement in field application.

Acknowledgement

This work is conducted under the Center of Reliable Power Electronics (CORPE) and Intelligent Efficient Power Electronics (IEPE) project framework at Aalborg University, Denmark.

9 References

- [1] Liserre, M.; Cardenas, R.; Molinas, M.; Rodriguez, J.: Overview of multi-MW wind turbines and wind parks. *Industrial Electronics*, IEEE Transactions on. Vol. 58, no. 4, pp. 1081-1095, 2011.
- [2] Blaabjerg, F.; Liserre, M.; Ke, M.: Power electronics converters for wind turbine systems. *Industry Applications*, IEEE Transactions on. Vol. 48, no. 2, pp. 708-719, 2012.
- [3] Chen, Z.; Guerrero, J.M.; Blaabjerg, F.: A review of the state of the art of power electronics for wind turbines. *Power Electronics*, IEEE Transactions on. Vol. 24, no. 8, pp. 1859-1875 2009.
- [4] Pedersen, K.,B.; Pedersen, K.: Bond wire lift-off in IGBT modules due to thermomechanical induced stress. *Power Electronics for Distributed Generation Systems (PEDG)*, 2012 3rd IEEE International Symposium on. PP. 519-526, 2012.
- [5] Ciappa, C.: Selected failure mechanisms of modern power modules. *Microelectronics Reliability*. Vol. 42, no. 4-5, pp. 653-667, 2002.
- [6] Yang, S.; Bryant, A.; Mawby, P.; Xiang, D.; Ran, L.; Tavner, P.: An industry-based survey of reliability in power electronic converters. in *Energy Conversion Congress and Exposition. ECCE 2009. IEEE*. 2009, pp. 3151-3157.
- [7] Song, Y.; Wang, B.: Survey on reliability of power electronic systems. *Power Electronics*, IEEE Transactions on. Vol. 28, no. 1, pp. 591-604 2013.
- [8] Bartram, M.; Von Bloh, J.; De Doncker, R.W.: Doubly-fed-machines in wind-turbine systems: is this application limiting the lifetime of IGBT-frequency-converters? in *Power Electronics Specialists Conference, 2004. PESC 04. 2004 IEEE 35th Annual*. 2004, pp. 2583-2587 Vol.4.
- [9] Smet, V.; Forest, F.; Huselstein, J.-.; Richardeau, F.; Khatir, Z.; Lefebvre, S.; Berkani, M.: Ageing and failure modes of IGBT modules in high-temperature power cycling. *Industrial Electronics*, IEEE Transactions on. Vol. 58, no. 10, pp. 4931-4941 2011.
- [10] Patil, N.; Celaya, J.; Das, D.; Goebel, K.; Pecht, M.: Precursor parameter identification for insulated gate bipolar transistor (IGBT) prognostics. *Reliability*, IEEE Transactions on. Vol. 58, no. 2, pp. 271-276 2009.
- [11] Ghimire, P.; Beczkowski, S.; Munk-Nielsen, S.; Rannestad, B.; Thøgersen, P.B.: A review on real time physical measurement techniques and their attempt to predict wear-out status of IGBT. *EPE'13 ECCE Europe 15th European Conference on Power Electronics and Applications*, Lille, France. Sep. 2013. In press.
- [12] Schmidt, R.; Scheuermann, U.: Using the chip as a temperature sensor — The influence of steep lateral temperature gradients on the Vce(T)-measurement. in *Power Electronics and Applications, 2009. EPE '09. 13th European Conference on*. 2009, pp. 1-9.
- [13] R.O. Nielsen, J. Due and S. Munk-Nielsen, "Innovative measuring system for wear-out indication of high power IGBT modules," in *Energy Conversion Congress and Exposition (ECCE), 2011 IEEE*, 2011, pp. 1785-1790.
- [14] Beczkowski, S.; Ghimire, P.; de Vega, A.R.; Munk-Nielsen, S.; Rannestad, B.; Thøgersen, P. B.: Online Vce measurement method for wear out monitoring of high power IGBT modules. *EPE'13 ECCE Europe 15th European Conference on Power Electronics and Applications*, Lille, France. Sep. 2013. In press.
- [15] Olesen, K.; Bredtmann, R.; Eisele, R.: "ShowerPower" New Cooling Concept for Automotive Applications, 2006.
- [16] Schilling, O.; Schfer, M.; Mainka, K.; Thoben, M.; Sauerland, F.: *Microelectronics Reliability*, vol. 52, pp 2347-2352, 2012.
- [17] Pedersen, K.B.; Pedersen, K.: Dynamical Modelling Method of Electro-Thermo-Mechanical Fatigue in IGBT Modules. To be published.
- [18] Codina, R.: *Computer Methods in Applied Mechanics and Engineering*, vol. 156, pp 185-210, 1998.
- [19] Filipis, S.; Kock, H.; Nelhiebel, M.; Kosel, V.; Decker, S.; Glavanovic, M.: *Microelectronics Reliability*, vol. 52, pp 2374-2379, 2012.
- [20] Rajapakse, A.; Gole, A.; Wilson, P.: Approximate loss formulae for estimation of IGBT switching losses through emp type simulations, *IEEE*, 2005.
- [21] Lutz, U.; Scheuermann, U.; Doncker, R.; Schlangenotto, R.: *Semiconductor Power Devices – Physics, Characteristics, Reliability*, Springer-Verlag, 2011.